

Mechanism of the benzidine disproportionation of (arylhydrazo)pyridines. The reactions of 4-(4-chlorophenylazo)pyridine and -hydrazo)pyridine in acid media

Robin A. Cox, Kap-Soo Cheon, Sam-Rok Keum, and Erwin Buncel

Abstract: A kinetic and product analysis study of the reactions of 4-(4-chlorophenylhydrazo)pyridine (**1**) and 4-(4-chlorophenylazo)pyridine (**2**) in acid media is reported. The disproportionation of two moles of **1** in aqueous sulfuric acid gives one mole of the oxidized product **2**, and one mole each of the reduced products 4-chloroaniline and 4-aminopyridine. The azo compound **2**, a product of the reaction of **1**, undergoes a slower hydroxylation reaction in acid media, and this process was also investigated. The first-formed product in the reaction of **2** is probably 4-(4-hydroxyphenylazo)pyridine, the 4-chlorine being displaced. At the low substrate concentrations used for the kinetic measurements both reactions are straightforward, but at the much higher concentrations used for product isolation studies a complex product mixture results, one of the products being a dimer. The complexity is increased because **1** had to be used as its hydrochloride salt for reasons of stability, and the chloride ion can also react with the diprotonated substrates; chloride ion also accumulates in the system as it is displaced from **2** during the hydroxylation. Thus chloride ion competes with bisulfate ion (present in large excess) for the diprotonated substrates. Nevertheless, complete mechanistic schemes accounting for all of the observed products, including the dimer, could be derived and are presented. Values of $pK_{BH_2^+}$ for **2** and two of the azo products, needed for the kinetic analysis, were measured using the excess acidity equilibrium method. The nucleophile reacting with protonated **2** in the rate-determining step of the hydroxylation was positively identified as being bisulfate ion by an excess acidity analysis. A comparison of the reaction of **1** with the equivalent reactions of two previously studied 4-(arylhydrazo)pyridines, **9** and **10**, reveals that the benzidine disproportionation of these molecules is an A1 process with the second protonation being a pre-equilibrium; $pK_{BH_2^+}$ values for the hydrazo compounds could not be measured as they react too quickly, but they could be determined from the kinetic data, using the excess acidity method. The rate-determining step is a thermally allowed 10-electron electrocyclic process of the diprotonated substrate, giving rise to an intermediate that undergoes fast reaction with a molecule of protonated substrate in a thermally allowed 14-electron electrocyclic process to give the observed products.

Key words: azopyridines, benzidine, disproportionation, excess acidity, hydrazopyridines, hydroxylation, mechanism.

Résumé : On a réalisé une étude cinétique ainsi qu'une analyse des produits des réactions des 4-(4-chlorophénylhydrazo)pyridine (**1**) et 4-(4-chlorophénylazo)pyridine (**2**) en milieu acide. La dismutation de deux molécules de **1** dans de l'acide sulfurique conduit à une mole du produit oxydé **2** et à une mole chacun des produits réduits, 4-chloroaniline et 4-aminopyridine. En milieu acide, le composé azo **2**, un produit de la réaction de **1**, subit une réaction d'hydroxylation plus lente; on a aussi examiné ce processus. Le premier produit formé dans la réaction de **2** est probablement la 4-(4-hydroxyphénylhydrazo)pyridine (**1**) provenant d'un remplacement du chlore en position 4. Aux faibles concentrations utilisées dans les mesures cinétiques, les deux réactions sont simples; toutefois, aux concentrations plus élevées utilisées pour les études en vue d'isoler les produits, il y a formation d'un mélange complexe de produits comprenant un dimère. La complexité est accrue à cause du fait qu'il a été nécessaire, pour des raisons de stabilité, d'utiliser le chlorhydrate du composé **1** et que l'ion chlorure peut aussi réagir avec les substrats diprotonés; de plus, l'ion chlorure s'accumule aussi dans le système lorsqu'il est déplacé du composé **2** par hydroxylation. L'ion chlorure est donc en compétition avec l'ion bisulfate (présent en très grand excès) pour les substrats diprotonés. Malgré tout, on peut présenter des schémas mécanistiques complets permettant d'expliquer tous les produits observés, y compris le dimère. Utilisant la méthode d'équilibre d'acidité en excès, on a mesuré les valeurs de $pK_{BH_2^+}$ du composé **2** et de deux produits azo nécessaires pour l'analyse cinétique. Faisant appel à l'analyse de

Received January 14, 1998.

This paper is dedicated to Professor Erwin Buncel in recognition of his contributions to Canadian chemistry.

R.A. Cox.¹ Department of Chemistry, University of Toronto, 80 St. George Street, Toronto, ON M5S 3H6, Canada.

K.-S. Cheon and E. Buncel.² Department of Chemistry, Queen's University, Kingston, ON K7L 3N6, Canada.

S.-R. Keum. Department of Chemistry, Graduate Studies of Korea University, Seoul, Korea 136-701.

¹ Mechanistic studies in strong acids, part 24. Part 23 is ref. 26. Telephone: (416) 978-4581. Fax: (416) 978-8775. E-mail: rcox@alchemy.chem.utoronto.ca

² Studies of azo and azoxy dyestuffs, part 25; part 24 is ref. 24. Telephone: (613) 545-2653. Fax: (613) 545-6669. E-mail: buncel@chem.queensu.ca

l'acidité en excès, il a été possible d'identifier sans ambiguïté que l'ion bisulfate est le nucléophile qui réagit avec la forme protonée de **2** dans l'étape cinétiquement limitante de l'hydroxylation. Une comparaison de la réaction de **1** avec les réactions équivalentes de deux 4-(arylhazopyridines (**9** et **10**) étudiées antérieurement révèle que la dismutation de la benzidine de ces molécules est un processus A1 dans lequel la deuxième protonation est un prééquilibre; il n'a pas été possible de mesurer les valeurs des $pK_{BH_2^+}$ de ces composés hydrazo à cause de leur trop grande vitesse de réaction, mais il a été possible de les déterminer à partir de données cinétiques faisant appel à la méthode d'acidité en excès. L'étape cinétiquement limitante est un processus électrocyclique thermique permis, à 10 électrons, du substrat diprotoné qui conduit à un intermédiaire qui réagit rapidement avec une molécule de substrat protoné par le biais d'un processus électrocyclique thermique permis, à 14 électrons, conduisant aux produits observés.

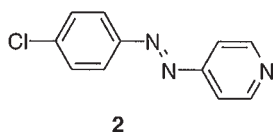
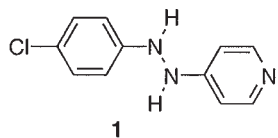
Mots clés : azopyridines, benzidine, dismutation, acidité en excès, hydrazopyridines, hydroxylation, mécanisme.

[Traduit par la rédaction]

Introduction

Studies of azo and azoxy compounds have revealed a remarkable diversity of structure–reactivity relationships, and some challenging problems in mechanism. Our work in this area was originally concerned with the mechanism of the acid-catalyzed Wallach rearrangement of azoxyarenes (1–7). This has developed in recent years to encompass a variety of photoactive molecules and processes, including the synthesis (8) and electronic spectral characteristics (9) of novel azo merocyanine dyes, and their solvatochromism (9, 10), which led to the establishment of the π^*_{azo} solvent polarity scale (10). The photochemical and thermal interconversion of merocyanines and their spiro precursors (11–15) has led most recently to studies of the chiroptical properties of spiro molecules, with a view to developing a ferroelectric liquid crystal optical switch based on the principle of photoresolution (16, 17).

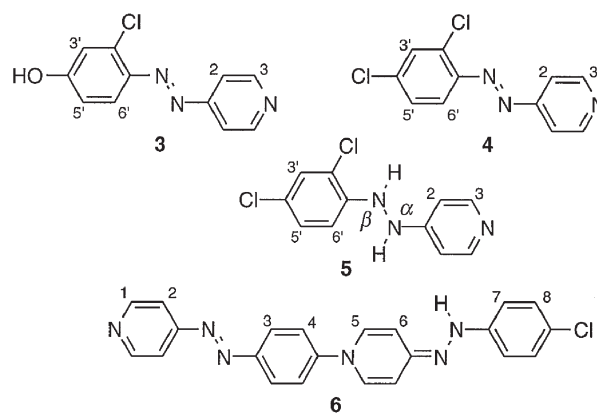
The present series of studies is an extension of the Wallach rearrangement studies of phenyl and naphthyl substrates (2–6) to the heteroaromatic series, with the observed $>10^4$ reactivity difference between the isomeric α - and β -phenylazopyridines involving di- and tri-protonation processes in the 95–100 wt.% H_2SO_4 acidity region (7). This led to the discovery of the remarkably facile hydrolysis of the aryl azo ethers in acid media, with protonation on nitrogen, oxygen or carbon centers occurring as fast equilibria or as the rate-determining step (18, 19). In the course of these studies it was discovered that phenylazopyridine is itself unstable in strong acid media, undergoing hydroxylation and disproportionation (20). Since this was reminiscent of the classical benzidine rearrangement (21–23), kinetic studies were extended to the surmised intermediate, 4-(4-hydroxyphenylhydrazo)pyridine (24). However, an excess acidity treatment of the results (25) led to uncertainties in the postulated reaction mechanism. This was unsatisfactory, since the excess acidity method (25) has proven to be very useful in the determination of the mechanisms of reactions that take place in strong acid media. For instance, lactam (26), alkylnitramine (27), *N*-nitro amide (28), and acylimidazole (29) hydrolyses, as well as imidazoline cyclizations (30), alkene hydrations (31), aromatic hydrogen exchange processes (32), and ether (19, 33) and thioacetal (34) hydrolyses have been studied using this approach.



Thus, in our quest to resolve the mechanistic ambiguity in the benzidine-type disproportionations of the 4-(arylhazopyridines (24), we have extended these studies to include 4-(4-chlorophenylhydrazo)pyridine **1**. We also examined the azo analog **2**, the results for which can be compared with those previously obtained for other (arylo)pyridines (20). These substrates form the subject of the present paper; it will be shown that while the results obtained using **1** and **2** are more complex in terms of reaction products, the kinetic data obtained do, in fact, allow the definitive resolution of the mechanism of this benzidine rearrangement-like process.

Experimental

The hydrochloride salt of 4-(4-chlorophenylhydrazo)pyridine **1** was obtained in 33.8% yield when 4-phenylazopyridine was simultaneously chlorinated and reduced (35), mp 241–242°C (lit. (35) mp 243°C). This compound was used as its hydrochloride salt rather than in the free base form, since the former proved to be much more air-stable. 4-(4-Chlorophenylazo)pyridine **2** resulted in 22.3% yield when **1** was oxidized (35), mp 97–98°C (lit. (35) mp 99–100°C). The synthesized compounds were characterized as before (20).



Substrates and isolated products were purified by several techniques, recrystallization, and column and thin-layer chromatography using silica gel 60 F₂₅₄ plates (BDH) in various eluting solvent systems. The products of the reactions of **1** and **2** in 65 wt.% aqueous H_2SO_4 were identified by UV–vis, NMR, and GC–MS analysis following direct isolation as previously described (20); some of the isolated products, **3–6**, are shown above. The MS results were particularly useful for

Table 1. Isolated products and yields in the reactions of **1** and **2** in 65 wt.% H₂SO₄.

Substrate	Product	Yield, %	Total yield, % ^a
1 (5 h)	4-(4-Chlorophenylazo)pyridine 2	22	48
	4-Aminopyridine	23	
	4-Chloroaniline	21	
	4-(2,4-Dichlorophenylhydrazo)pyridine 5	4	
1 (24 h)	4-(2,4-Dichlorophenylazo)pyridine 4	21	50
	4-Aminopyridine	25	
	2,4-Dichloroaniline	20	
	4-(4-Chlorophenylazo)pyridine 2	5	
	4-Chloroaniline	3	
	Dimeric product 6	Trace	
2	4-(2-Chloro-4-hydroxyphenylazo)pyridine 3	15	57
	4-(2,4-Dichlorophenylazo)pyridine 4	13	
	2-Chloro-4-hydroxyaniline	14	
	4-Aminopyridine	26	
	2,4-Dichloroaniline	10	
	4-(4-Hydroxyphenylazo)pyridine 7	2	
	Dimeric product 6	2	

^a Since two aniline products result from one substrate molecule, their yields have to be averaged in calculating the overall yield, which is why the numbers in this column are not the simple sum of those in the previous column.

identifying the chlorine-containing products; for instance, the mass spectrum of **4** with its two chlorine atoms showed a characteristic intensity pattern of 100:65.3:10.6, in which each peak is separated by two mass units due to the natural abundance of the two chlorine isotopes, ³⁵Cl:³⁷Cl being 100:32.5. The structural identification of the products was achieved using ¹H NMR spectroscopy and MS. For **3**: δ_H (DMSO-*d*₆): 12.82 (OH), 8.79 (H³), 7.83 (H²), 7.68 (H⁶), 7.17 (H^{3'}), 6.98 (H^{5'}); *m/z*: 233.0 (M). For **4**: δ_H (DMSO-*d*₆): 8.86 (H³), 7.96 (H^{3'}), 7.77 (H²), 7.73 (H⁶), 7.60 (H^{5'}); *m/z*: 251.0 (M). For **5**: δ_H (DMSO-*d*₆): 8.90 (NH^α), 8.14 (H³), 8.08 (NH^β), 7.48 (H^{3'}), 7.20 (H^{5'}), 6.74 (H⁶), 6.67 (H²); *m/z*: 235.1 (M). For the dimer **6**: δ_H (DMSO-*d*₆): 9.98 (NH), 8.72 (H¹), 8.14 (H⁵), 7.86 (H³), 7.65 (H²), 7.42 (H^{7,8}), 7.16 (H⁴), 6.60 (H⁶); *m/z*: 401.2 (M+1).

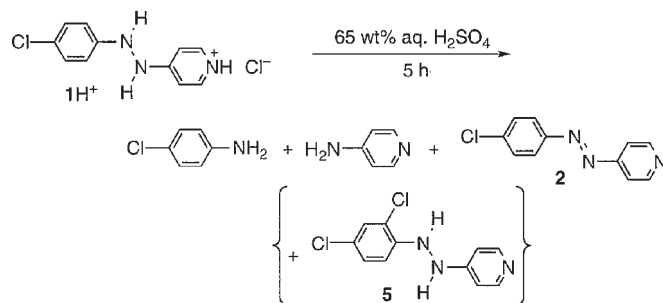
The p*K*_{BH₂⁺} values of the azo substrate **2** and the azo products **3** and **4** were determined from the variation of the UV–vis spectra with sulfuric acid concentration as previously described (20); the acid concentration and extinction data are given here as supplementary information, Tables S1–S3.³ The kinetic techniques used were similar to those used before (20).

Results

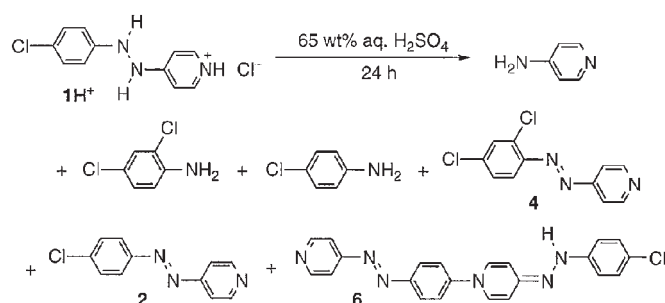
Products

The products formed when 4-(4-chlorophenylhydrazo)pyridine **1** is allowed to react in 65 wt.% H₂SO₄ for 5 h at a substrate concentration of 0.05 M are given in Table 1, and illustrated in Scheme 1. Under these conditions, and at the much lower substrate concentrations used for the kinetic runs (as determined from the UV–vis spectra after the kinetic runs), the reaction gives the three products shown, 4-(4-chlorophenylazo)pyridine **2**, 4-chloroaniline, and 4-aminopyridine. Trace

Scheme 1.



Scheme 2.

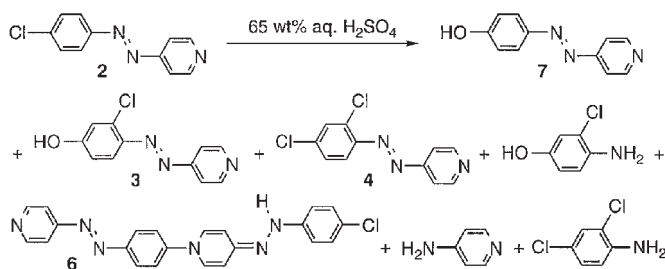


amounts of 4-(2,4-dichlorophenylhydrazo)pyridine **5** were also present in the mixture analyzed.

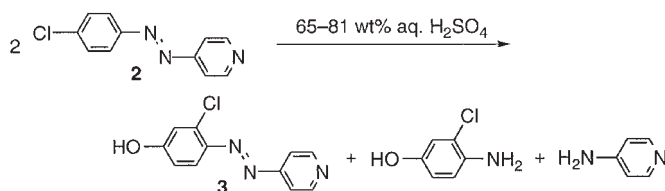
If the reaction of **1** is allowed to continue for longer periods the number of products increases, as shown in Table 1 and illustrated in Scheme 2. The products still include **2**, 4-chloroaniline, and 4-aminopyridine, but 4-(2,4-dichlorophenylazo)pyridine **4** and 2,4-dichloroaniline are also present, with trace amounts of the dimeric product **6**. There is no evidence for the presence of **5**, leading to the inference that at least some of the new products may have been formed from it. The presence of extra Cl⁻ (**1** had to be used as its hydrochloride salt)

³ Tables S1–S3, supplementary material, may be purchased from: The Depository of Unpublished Data, Document Delivery, CISTI, National Research Council of Canada, Ottawa, Canada, K1A 0S2.

Scheme 3.



Scheme 4.



also complicates the situation. The product recovery in Table 1 is less than 100%, probably due to losses incurred during the TLC technique used for product separation (20).

The first-formed product **2** also reacts in aqueous H_2SO_4 , albeit more slowly than does **1**, and the products of the reaction of **2** at 0.05 M substrate concentration were also investigated, see Table 1. A complex mixture of **4**, 4-(2-chloro-4-hydroxyphenylazo)pyridine **3**, 4-(4-hydroxyphenylazo)pyridine **7**, 2-chloro-4-hydroxyaniline, 2,4-dichloroaniline, 4-aminopyridine, and the dimeric product **6** was found, as shown in Scheme 3.

However, at the substrate concentrations typically used for the kinetic runs, $\sim 8 \times 10^{-5}$ M, the situation for **2** is much simpler, as shown in Scheme 4. The primary product is **3**, which could be identified by its UV–vis spectrum; the concentration of this product was shown not to depend on the medium acidity, averaging $(46.8 \pm 4.0)\%$ over the 65–81 wt.% H_2SO_4 concentration range, as determined from the known extinction coefficients and the observed absorbances after 10 half-lives. The two aniline products also formed could not be directly identified, but undoubtedly form in equivalent amounts (20). Evidently the reaction is uncomplicated; according to Table 1 two moles of **2** give one mole of oxidized products (total 30% azo compounds) and one mole of reduced products with the N–N bond broken (total 24% anilines, 26% 4-aminopyridine).

 $pK_{\text{BH}_2^{2+}}$ values

The azo compounds **2–4** are all protonated on the pyridine nitrogen in the pH range (8), so the protonation of interest in this work is the second protonation at the azo group. The $pK_{\text{BH}_2^{2+}}$ values were measured as described before (20). Extinction differences ($\delta\epsilon = \epsilon_{\text{BH}^+} - \epsilon_{\text{BH}_2^{2+}}$) were obtained from UV–vis spectra measured in different sulfuric acid solutions at wavelengths appropriate for the peak maxima of the protonated and diprotonated forms; this is the Davis–Geissman method (36), preferred because errors due to small differences between the individual samples tend to cancel out when the difference is taken (these may cause irregular isosbestic point

Table 2. Azo-compound $pK_{\text{BH}_2^{2+}}$ values obtained using the excess acidity method.^a

Compound	Substituents	$pK_{\text{BH}_2^{2+}}$	m^*
2	4-Cl	-6.47 ± 0.37	0.991 ± 0.070
3	4-OH, 2-Cl	-4.15 ± 0.26	0.760 ± 0.063
4	2,4-Di-Cl	-6.61 ± 0.32	0.875 ± 0.053
7^b	4-OH	-3.07 ± 0.21	0.994 ± 0.089
8^b	H	-4.97 ± 0.22	0.807 ± 0.045

^a Errors quoted are standard deviations.

^b From ref. 20.

behaviour, for instance), and spectra of both forms contribute to the resulting $pK_{\text{BH}_2^{2+}}$ values. The data were treated according to the excess acidity method; for equilibria the relevant equation is $\log I - \log C_{\text{H}^+} = pK_{\text{BH}_2^{2+}} + m^*X$ (37), where C_{H^+} is the proton concentration in the sulfuric acid solution and X is the excess acidity, both obtained from published sources (37). The ionization ratio I is given in terms of $\delta\epsilon$ by $I = (\delta\epsilon_{\text{BH}^+} - \delta\epsilon)/(\delta\epsilon - \delta\epsilon_{\text{BH}_2^{2+}})$ (38), where $\delta\epsilon_{\text{BH}^+}$ and $\delta\epsilon_{\text{BH}_2^{2+}}$ apply to the pure monoprotonated form and the pure diprotonated form, respectively. This expression was substituted in the excess acidity equation and the result recast in terms of $\delta\epsilon$ and curve-fitted directly, as before (38); previous experience (39) shows that this method gives reliable protonation constants. The slope parameter m^* is characteristic of the substrate, having values of 1.0 for primary nitroanilines, 0.6 for amides and so on (37). The parameters given by the curve fit are $\delta\epsilon_{\text{H}^+}$, $\delta\epsilon_{\text{BH}_2^{2+}}$, $pK_{\text{BH}_2^{2+}}$, and m^* ; the latter two are listed for **2–4** in Table 2. Also listed in Table 2 are the $pK_{\text{BH}_2^{2+}}$ and m^* values for 4-(4-hydroxyphenylazo)pyridine **7** and the parent compound **8**, already available (20), for comparison. The experimental data obtained and the values of X and $\log C_{\text{H}^+}$ used for **2–4** are given as supplementary material in Tables S1–S3,³ together with the calculated $\delta\epsilon_{\text{BH}^+}$ and $\delta\epsilon_{\text{BH}_2^{2+}}$ values.

Kinetics

The kinetics of the reaction of 4-(4-chlorophenylazo)pyridine **2** (see Scheme 4) were monitored spectrophotometrically by following the disappearance of the reactant, in either its monoprotonated SH^+ form at 354 nm (up to 72 wt.% H_2SO_4), or its diprotonated SH_2^{2+} form at 444 nm (at the higher acidities). The observed pseudo-first-order rate constants as a function of acidity, k_{ψ} , and other parameters relevant to the kinetic analysis, are given in Table 3. All the kinetic plots showed excellent first-order linearity over the three half-lives for which the reaction was typically followed.

$$[1] \quad \log k_{\psi} - \log (C_{\text{SH}_2^{2+}} / (C_{\text{SH}^+} + C_{\text{SH}_2^{2+}})) - \log a_{\text{Nu}^-} \\ = \log k_0 + (m^{\ddagger} - 1)m^* X$$

Previously it was found that eq. [1] describes the kinetic behaviour of 4-(phenylazo)pyridine (**8**) (and that of 2-(phenylazo)pyridine) at these acidities (20), and the behaviour of **2** was found to be very similar. Protonation of the substrate is a pre-equilibrium process (20), and so the $pK_{\text{BH}_2^{2+}}$ and m^* values given in Table 2 were used with the equilibrium excess acidity equation to calculate protonation correction terms (PCT) on the basis of full substrate protonation, $\log (C_{\text{SH}_2^{2+}} / (C_{\text{SH}^+} + C_{\text{SH}_2^{2+}}))$, or $\log (I/(1 + I))$ after division by C_{SH^+} (since the ionization ratio $I = C_{\text{BH}_2^{2+}} / C_{\text{BH}^+}$), which correct

Table 3. Kinetic data for the hydroxylation of 4-(4-chlorophenylazo)pyridine **2**.

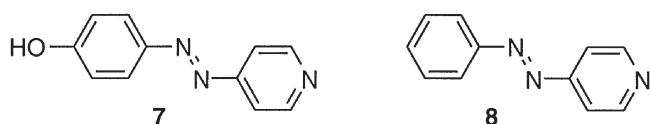
H ₂ SO ₄ , wt. %	k_{ψ}^a	X^b	$\log C_{H^+}^b$	$\log C_{\text{HSO}_4^-}$	PCT ^c	$\log k_{\psi}$ - PCT
64.99	2.01	3.793	1.078	0.932	-1.640	-3.057
	2.03					-3.053
68.22	2.90	4.208	1.100	0.975	-1.224	-3.314
	2.91					-3.312
71.67	7.32	4.708	1.122	1.020	-0.762	-3.373
	7.35					-3.372
75.86	9.12	5.397	1.144	1.071	-0.289	-3.751
	9.16					-3.749
78.28	7.99	5.830	1.154	1.096	-0.128	-3.969
	8.01					-3.968
81.36	3.91	6.407	1.157	1.118	-0.038	-4.370
	3.92					-4.369
85.98	0.81	7.274	1.118	1.102	-0.006	-5.086
	0.81					-5.086

^a Observed pseudo-first-order rate constants, $\times 10^5 \text{ s}^{-1}$. Both duplicate determinations given.

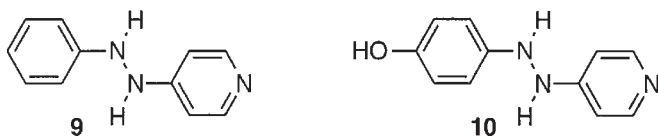
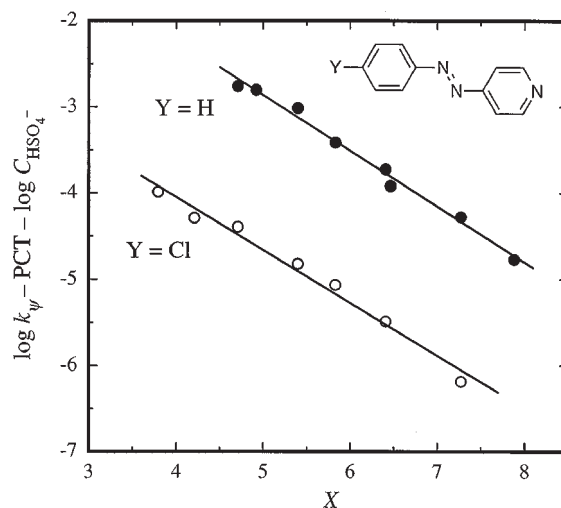
^b From ref. 37.

^c Protonation Correction Term; $\log (C_{\text{SH}_2^{2+}} / (C_{\text{SH}^+} + C_{\text{SH}_2^{2+}}))$. Calculated using $\text{p}K_{\text{BH}_2^{2+}} = -6.47$ and $m^* = 0.991$ from Table 2.

for less than full substrate protonation at the acidity under investigation. The nucleophile involved at these acidities is bisulfate ion, and \log bisulfate ion concentrations were used for $\log a_{\text{Nu}^-}$ as before (20). $\log k_0$ refers to the rate constant for the reaction in the hypothetical ideal 1 M acid solution which is the standard state (37), and m^{\ddagger} refers to the transition state, having values of >1 for an A1 reaction, <1 for an A-S_E2 reaction, and probably ~ 1 for an A2 reaction with water (25). Plots according to eq. [1] are given in Fig. 1 for **2**, with that for the parent compound **8** for comparison (20). For the reaction of **8** with bisulfate, $\log k_0 = 0.36 \pm 0.11$ and $m^*(m^{\ddagger} - 1) = -0.645 \pm 0.018$, i.e. $m^{\ddagger} = 0.201 \pm 0.050$ (20). In this work we find, for the reaction of **2** with bisulfate, $\log k_0 = -1.60 \pm 0.13$ and $m^*(m^{\ddagger} - 1) = -0.612 \pm 0.024$, i.e. $m^{\ddagger} = 0.383 \pm 0.031$.



The kinetics of the disproportionation of **1** could be conveniently followed spectrophotometrically over the 60–86 wt. % H₂SO₄ range, by monitoring the formation of the azo product, 4-(4-chlorophenylazo)pyridine **2** (see Scheme 1) at either 354 nm (up to 72 wt. % H₂SO₄, monoprotonated form) or at 444 nm (at the higher acidities, diprotonated form). Reactions were generally followed over three half-lives, and all showed excellent first-order behaviour over this range. The observed pseudo-first-order rate constants, k_{ψ} , are given in Table 4, together with other pertinent information.

**Fig. 1.** Excess acidity plots for the reactions of **2** (open circles) and **8** (closed circles) (20) in aqueous sulfuric acid, assuming reaction with one bisulfate ion.**Table 4.** Kinetic data for the disproportionation of 4-(4-chlorophenylazo)pyridine **1**.

H ₂ SO ₄ , wt. %	k_{ψ}^a	X^b	$\log C_{H^+}^b$	PCT ^c	$\log k_{\psi}$ -PCT
59.96	0.0384	3.234	1.039	-0.644	-3.772
	0.0386				-3.769
64.99	0.162	3.793	1.078	-0.270	-3.520
	0.163				-3.518
68.22	0.362	4.208	1.100	-0.119	-3.322
	0.363				-3.321
71.67	0.839	4.708	1.122	-0.039	-3.037
	0.843				-3.035
75.86	2.02	5.397	1.144	-0.008	-2.687
	2.02				-2.687
78.28	3.01	5.830	1.154	-0.003	-2.518
	3.05				-2.513
81.36	5.44	6.407	1.157	-0.001	-2.263
	5.48				-2.260
85.98	16.7	7.274	1.118	0	-1.777
	16.9				-1.772

^a Observed pseudo-first-order rate constants, $\times 10^3 \text{ s}^{-1}$. Both duplicate determinations given.

^b From ref. 37.

^c Protonation Correction Term; $\log (C_{\text{BH}_2^{2+}} / (C_{\text{BH}^+} + C_{\text{BH}_2^{2+}}))$. Calculated using the $\text{p}K_{\text{BH}_2^{2+}}$ value of -4.806 ($m^* = 1$) given in Table 5.

These rate data were also treated according to the excess acidity method (25). To this end plots of $\log k_{\psi} - \log C_{H^+}$ vs. X for **1**, together with the previously published equivalent plots for the parent 4-(phenylazo)pyridine **9** and 4-(4-hydroxyphenylazo)pyridine **10** for comparison (24), are shown here as Fig. 2. The observed downward curvature in Fig. 2 indicates (a) that the reaction is not an A-S_E2 process, as otherwise these plots would be straight, and (b) that the data go through a $\text{p}K_a$ value (substrate titration) in an A1 reaction, which means that a protonation correction term has to be applied (25). Reaction with water in an A2 process would also

Fig. 2. Excess acidity plots of $\log k_{\psi} - \log C_{H^+}$ vs. X for the reactions of **1** (open triangles), **9** (open circles) (24), and **10** (closed circles) (24) in aqueous sulfuric acid, illustrating the downward curvature due to substrate titration. The points are experimental and the curves theoretical, see text.

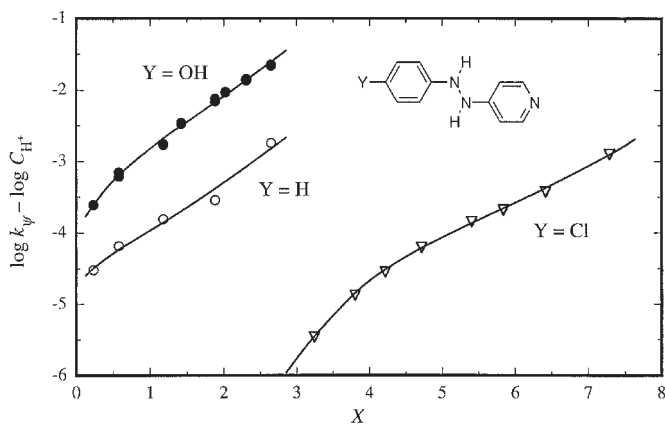


Table 5. Second basicities and excess acidity slopes and intercepts for the phenylhydrazopyridines **1**, **9**, and **10**.^a

Substrate	Substituents	$pK_{BH_2^{2+}}$	$\log k_0$	m^{\ddagger}
1	4-Cl	-4.806 ± 0.045	-5.371 ± 0.052	1.4915 ± 0.0092
9	H	-0.59 ± 0.45	-4.15 ± 0.52	1.87 ± 0.12
10	4-OH	-1.038 ± 0.090	-2.934 ± 0.098	1.872 ± 0.033

^a Errors listed are standard deviations.

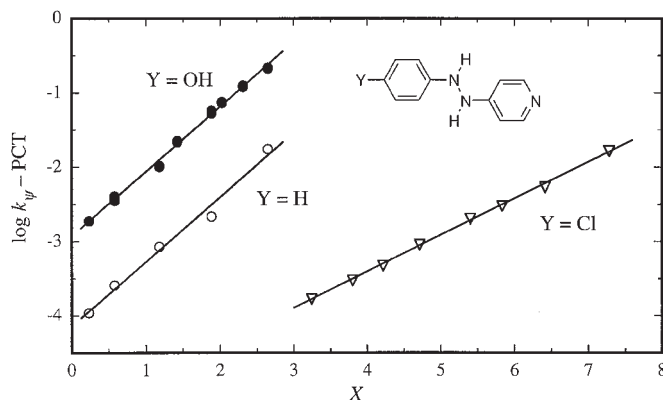
cause downward curvature in these plots (20, 27), but if that were the case here the curvature would be different for the different substrates, with much stronger curvature for **2** than for **10**, since the water activity decreases with acidity much faster at the higher acidities (4). The observed (Fig. 2) very similar curvature for **2** and **10** is much more likely to be due to a substrate titration; indeed, the Fig. 2 plots straighten out, as expected for a substrate protonation, rather than show the increasing curvature that would be expected for a reaction with water. This mechanistic distinction can now be made, with the addition of the data for **2**, whereas it could not without it (24).

The protonation involved is again the second one, undoubtedly on the hydrazo group, because these compounds are all already protonated on the pyridine ring, this process occurring in the pH range (8). The $pK_{BH_2^{2+}}$ values for these compounds are not known, and reaction is too fast to allow them to be measured, but $pK_{BH_2^{2+}}$ values can be estimated from the curvature of the kinetic plots in Fig. 2. It has recently been shown that quite precise values can be obtained in this way (29). The modified excess acidity equation for an A1 reaction that applies here, accounting for the changing state of protonation with acidity, is eq. [2] (25):

$$[2] \quad \log k_{\psi} - \log C_{H^+} - \log (C_{BH^+} / (C_{BH^+} + C_{BH_2^{2+}})) \\ = \log (k_0 / K_{BH_2^{2+}}) + m^{\ddagger} m^* X$$

where k_0 is the standard-state rate constant for the reaction. The protonation correction term in eq. [2], $\log (C_{BH^+} / (C_{BH^+} + C_{BH_2^{2+}}))$, becomes $\log (1 / (1 + I))$ upon division by C_{BH^+} , and we can put $m^* = 1$ in the excess acidity equation

Fig. 3. Excess acidity plots of $\log k_{\psi} - \log (C_{BH_2^{2+}} / (C_{BH^+} + C_{BH_2^{2+}}))$ (PCT) vs. X for the reactions of **1** (open triangles), **9** (open circles), and **10** (closed circles) in aqueous sulfuric acid.



for equilibria ($\log I = pK_{BH_2^{2+}} + m^* X + \log C_{H^+}$), because these hydrazo compounds are very similar to the H_0 primary aniline indicators, for which m^* is known to have the value 1.0 (37). Using eq. [2] means that we have three unknowns to calculate for each compound, slope ($m^{\ddagger} m^*$), intercept ($\log (k_0 / K_{BH_2^{2+}})$) and $pK_{BH_2^{2+}}$. A standard curve-fitting computer program was used (40), and the resulting, reasonably precise, $pK_{BH_2^{2+}}$ values are given in Table 5. These were then used to calculate protonation correction terms in the form $\log (C_{BH_2^{2+}} / (C_{BH^+} + C_{BH_2^{2+}}))$. Subtraction of the latter from $\log k_{\psi}$ results in the very good straight lines in Fig. 3. This figure is drawn on the basis of full substrate protonation, which more accurately reflects the true situation at these acidities. The slope is $(m^{\ddagger} - 1)m^*$ and the intercept is $\log k_0$ (25). These and the observed m^{\ddagger} values, with their errors, are also given in Table 5. The m^{\ddagger} values, all >1 , are only consistent with an A1 mechanism (25). The Table 5 values were used to calculate the theoretical curves in Fig. 2.

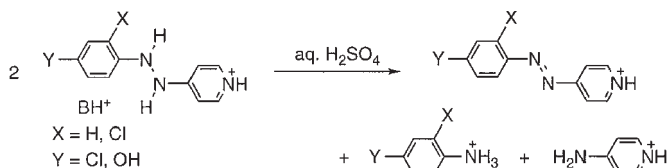
Discussion

Reaction pathways

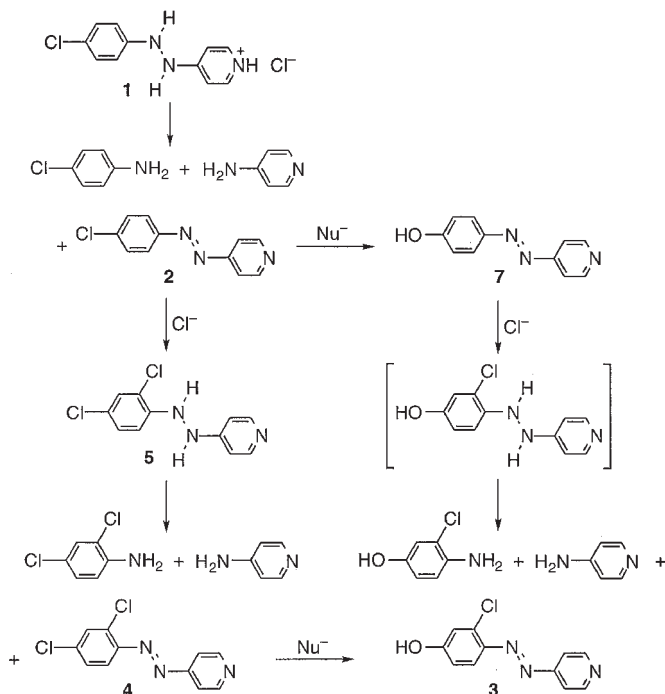
The products of the reactions of **1** and **2** in acid media, given in Table 1 and in Schemes 1–4, are quite complex. Although under kinetic conditions Schemes 1 and 4 prevail, it is nevertheless most convenient to begin with the elements that are common to several schemes. We have established previously (24) that 4-(phenylhydrazo)pyridines undergo a disproportionation in sulfuric acid media, for example, see Scheme 1, very similar to the processes undergone by other hydrazo compounds that have both 4-positions blocked (21, 41). Two substrate molecules give an azo compound (oxidized product) and two anilines (reduced products), as shown in Scheme 5. This disproportionation is much faster than any reaction undergone by the 4-(phenylazo)pyridine products (24); for the reactions of **1** and **2** this is readily apparent from a comparison of the rate constants in Tables 3 and 4. It is also very likely to be irreversible, since the reverse would be a termolecular process.

Deferring consideration of the mechanism until later, it is apparent that as soon as a hydrazo compound is formed it will react according to Scheme 5. The other products, apart from the dimer, can then be accounted for as shown in Scheme 6.

Scheme 5.



Scheme 6.

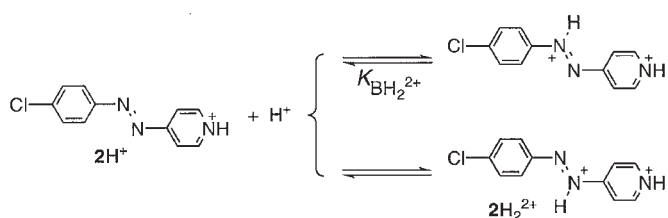


Starting with **1**, which has an equimolar amount of chloride ion present, product formation takes place from top to bottom on the left-hand side only, with no displacement by hydroxide occurring; products on the right are not observed if the starting material is **1**. On the other hand, if the starting material is **2** there is no free chloride ion present initially and the first reaction is $2 \rightarrow 7$, with subsequent product formation taking place down both sides of Scheme 6, chloride ion accumulating as it is displaced. The hydrazo product in brackets is the only one we did not observe, presumably because it is too reactive.

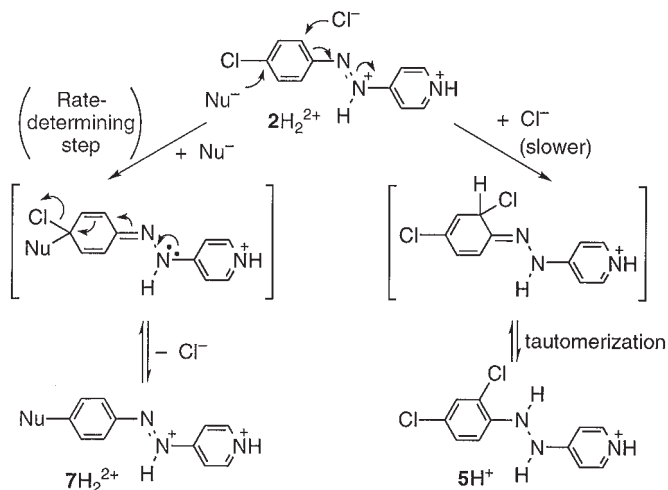
The reaction of 2H^+ begins with a second protonation (the reaction is acid catalyzed), undoubtedly on the azo group. There are two nitrogens that can be protonated, as shown in Scheme 7. It does not particularly matter which azo nitrogen bears the proton, since the nitrogen lone pairs do not form part of the π system, but it seems reasonable to place it on the nitrogen furthest from the pyridinium positive charge, and the $pK_{\text{BH}_2^{2+}}$ values quoted in Table 2 probably refer to this. However, it is easier to draw the mechanistic schemes for subsequent reactions with the proton on the other nitrogen, 2H_2^{2+} in Scheme 7.

Two different mechanistic possibilities for 2H_2^{2+} are given in Scheme 8. (In Scheme 8 and subsequently the attacking nucleophile is identified as either Cl^- or as Nu^- ; the latter is actually HSO_4^- in these media, as shown by the kinetic analysis

Scheme 7.



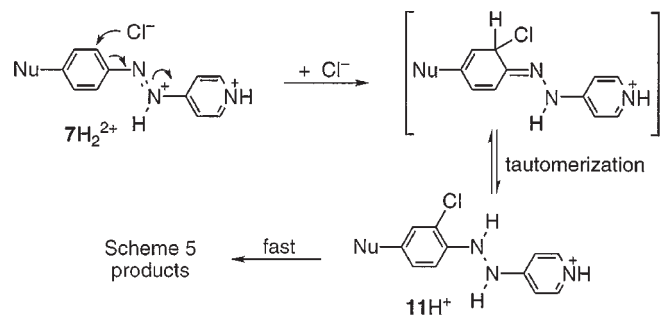
Scheme 8.



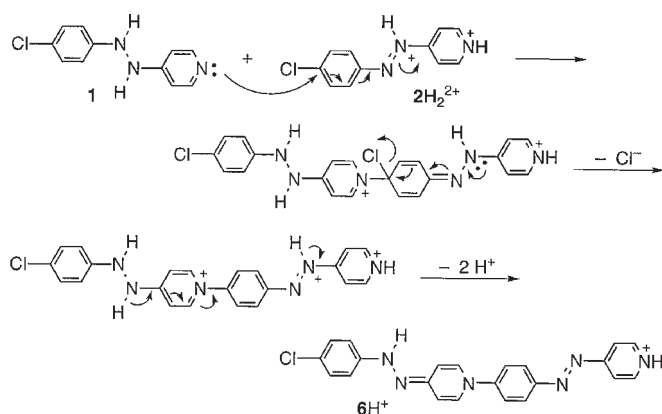
(see Fig. 1), but in the identified products it appears as OH, since these sulfate ester products hydrolyze very rapidly to phenols in more dilute acid, as we have shown previously (42), and this will occur during the product work-up.) Chloride ion is present during the reaction of **2** when it derives from **1**, since **1** had to be used as its hydrochloride salt, and it accumulates as Nu^- displaces it from **2**; it is the best nucleophile in the system, and can react at the 2-position of the phenyl group in 2H_2^{2+} as shown on the right-hand side of Scheme 8. Tautomerization leads to the hydrazo compound 5H^+ , most of which will react according to Scheme 5, giving the observed product **4** (Schemes 2 and 3). However, in the initial reaction of **2** itself the chloride concentration is zero, and thus the rate-determining step involves diprotonated **2** and bisulfate ion, as shown by the kinetic analysis; this is the left-hand pathway in Scheme 8. Loss of chloride ion (a good leaving group) as shown gives 7H_2^{2+} . With free chloride ion now present, the right-hand side of Scheme 8 can come into play, and 7H_2^{2+} can also react further, as shown in Scheme 9. Presumably the better nucleophile Cl^- can react at the more crowded *ortho* site (Schemes 8 and 9), whereas the far worse (and much bigger) nucleophile HSO_4^- is limited to *para* attack.

The chlorination of 7H_2^{2+} , shown in Scheme 9, will be faster than the chlorination of 2H_2^{2+} , shown at the right of Scheme 8, because of the presence of the inductively electron-withdrawing oxygen in the Nu group encouraging nucleophilic attack. Again, fast tautomerization leads to a hydrazo compound, 11H^+ , which will immediately react via Scheme 5 to give the observed product **3** (Schemes 3 and 4); in fact this is the first-formed major product in the reaction of **2**, according to the kinetics and Scheme 4. There are other possibilities; for

Scheme 9.



Scheme 10.

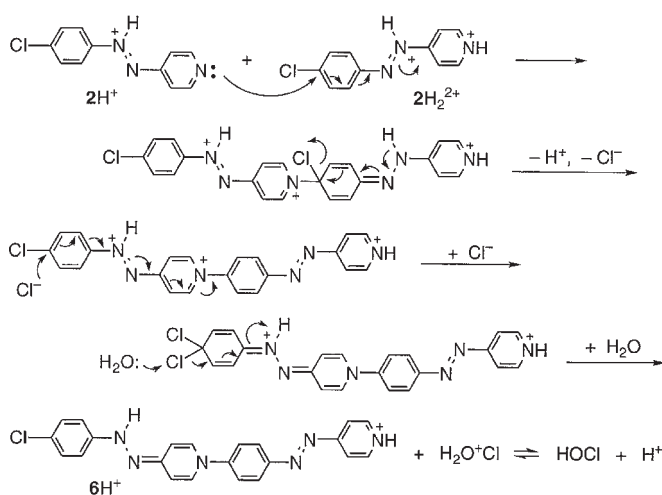


instance, it seems reasonable that 4H_2^{2+} could undergo a chlorine displacement as in Scheme 8 to give 3H_2^{2+} (and hence the isolated products should contain more **3** than **4**, see Table 1), and any two hydrazo compounds can take part in the disproportionation of Scheme 5. It is also possible (although probably less likely) that the 4-chloro- and 4-hydroxyanilinium ion products formed can be chlorinated at the 2-position by the free chloride ion (the presence of the $^+\text{NH}_3$ group increasing susceptibility to nucleophilic attack), perhaps giving rise to some of the observed 2,4-dichloro- and 2-chloro-4-hydroxyanilinium products.

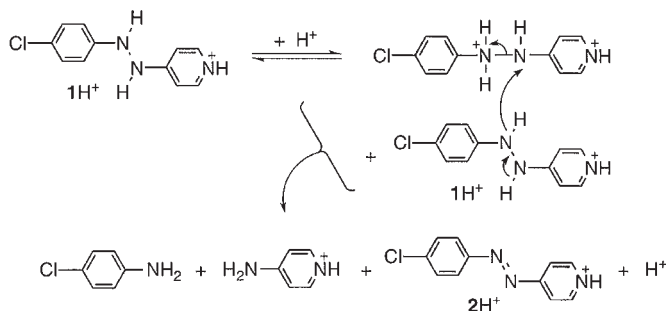
The only remaining major product to be accounted for is the dimer **6**. It has been mentioned that chloride ion is the best nucleophile in the system, but if any starting material that is not protonated on the pyridine nitrogen is present, this will be quite nucleophilic as well. The simplest dimerization possibility is a nucleophilic attack by **1** on 2H_2^{2+} , as shown in Scheme 10. (It is likely that **1** will be protonated somewhere on the hydrazo group; for simplicity it is shown as being unprotonated in Scheme 10.) Loss of chloride ion from the resulting intermediate is straightforward, and simple loss of two more protons gives the observed dimer product **6**.

Another possibility results from an attack of 2H^+ on 2H_2^{2+} , as shown in Scheme 11. Essentially, chlorine has to be lost as Cl^+ in this scheme, but this has precedence in reactions of this type; Rhee and Shine have observed a similar Cl^+ loss during the benzidine rearrangement and disproportionation of 4,4'-dichlorohydrazobenzene (43). Whatever the dimerization mechanism may be, presumably dimerization will diminish in importance as the acidity increases, since the probability of

Scheme 11.



Scheme 12.



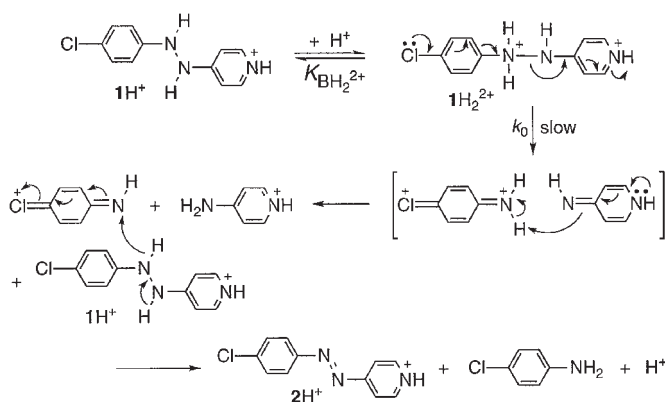
having an unprotonated pyridine nitrogen present decreases with increasing acidity, and, being bimolecular, the reaction will only occur at all at the high substrate concentrations used for the product analysis.

pK_a relationships

The $\text{pK}_{\text{BH}_2^{2+}}$ values for the various 4-(arylphenylazo)pyridines listed in Table 2 seem reasonable, with compounds having electron-donating OH groups being easier to protonate on the azo group, and those with electron-withdrawing Cl being more difficult. There are insufficient data for a good linear free energy relationship (some of the substituents are *ortho* in any case), but a ρ^+ value of -2.9 ± 0.6 can be estimated. The m^* slopes show considerable variation, averaging 0.86 ± 0.09 . The reactions undergone by **2** and **8** are not quite the same, that of **2** being an *ipso* substitution at a carbon already bearing a substituent but, as Fig. 1 shows, the kinetic behaviour is very similar, and reaction of the deactivated chloro compound is slower, by a factor of ~ 100 in the standard state according to the intercept difference.

The m^\ddagger values for both **2** and **8** are < 0.5 . At the moment

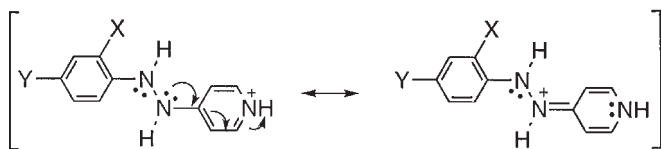
Scheme 13.



there are very few data for comparison, and so it is difficult to predict m^\ddagger values for reaction with bisulfate. In the case of protonated benzamide a value of 1.1 was found for nucleophilic attack of bisulfate at the carbonyl group (44) (but this number is subject to revision (26)), and for several substituted alkylnitramines values of m^*m^\ddagger between 0.9 and 1.2 were found for S_N2 displacement by bisulfate (27), the value of m^* unfortunately not being known. Neither case corresponds very well to the situation in the reaction under discussion here, nucleophilic attack on a benzene ring.

Benzidine disproportionation mechanism

Proposed mechanisms for the benzidine disproportionation of **1** (and the other 4-(phenylhydrazo)pyridines involved in this work) have to account for the observed kinetic behaviour, which is that the rate-determining step of these disproportionations is an A1 process involving the diprotonated substrate, as well as the reaction products. The second protonation is written as occurring on the hydrazo nitrogen away from the pyridinium ring. There are two reasons for this: apart from simple electrostatic repulsion of the two positive charges, the lone pair on the other nitrogen is occupied to some extent in resonance interaction with the pyridinium centre, as shown, and so is less available for protonation.

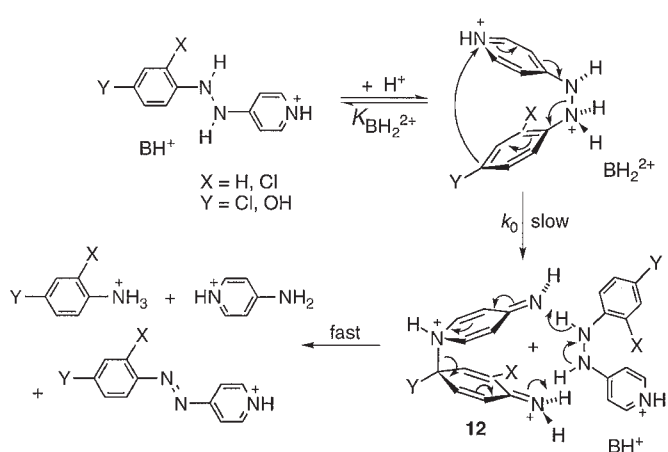


Processes such as the one shown in Scheme 12, although it gives the correct products, can be ruled out as Scheme 12 would result in second-order kinetics, and all of the observed kinetics were accurately first order, for **1** and also for **9** and **10** (24).

Scheme 13, involving rate-determining breakup of diprotonated $1H_2^{2+}$, is a more plausible mechanism. Deriving an excess acidity rate equation based on Scheme 13 is straightforward (25). On the basis of full substrate diprotonation, the observed rate constants k_ψ can be equated with k_0 and the activities of the species present in the activated complex according to eq. [3].

$$[3] \quad k_\psi (C_{BH^+} + C_{BH_2^{2+}}) = k_0 a_{BH_2^{2+}} / f_\ddagger$$

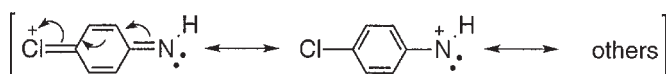
Scheme 14.



$$[4] \quad \log k_\psi - \log (C_{BH_2^{2+}} / (C_{BH^+} + C_{BH_2^{2+}})) = \log k_0 + (m^\ddagger - 1)m^* X$$

Upon replacing activity by concentration and activity coefficient, taking logs and rearranging, eq. [3] becomes eq. [4], since the log activity coefficient ratio term here is equal to $(m^\ddagger - 1)m^*$ (25), where the slope parameters m^* ($= 1$ in this case) and m^\ddagger are defined above. This is the rate equation that gives the good straight lines in Fig. 3.

Although Scheme 13 explains the products and the kinetics, there is a problem with it. The proposed chloronium intermediate is actually a nitrenium ion:



and these are highly reactive, with very short lifetimes (45). They have carbene-like properties, and would be expected to react almost instantly with the water present, probably on the aromatic ring (46). So Scheme 13 can be ruled out on the grounds that this nitrenium ion would not exist long enough for the suggested hydride transfer from another $1H^+$ molecule to be possible.

Thus the most likely mechanism for the reaction of **1**, **9**, and **10**, and the other hydrazo compounds suggested as intermediates in this work, is the benzidine-type disproportionation mechanism shown in Scheme 14 for the general structure BH^+ , as proposed previously (24). This would give the same kinetic behaviour as does Scheme 13, i.e., eq. [4] is followed. The rate-determining step is a thermally allowed 10-electron electrocyclic reaction involving the diprotonated substrate BH_2^{2+} , giving rise to intermediate **12**. This is now firmly established as being the key step in the rearrangement mechanism for hydrazobenzene and many other hydrazo aromatics, primarily by the application of heavy-atom isotope effect studies to these processes (21, 23). Also, for hydrazobenzene itself, an intermediate equivalent to **12** has been experimentally observed under stable-ion conditions (47). Regular hydrazo compounds can form benzidines by rearomatization of intermediates like **12**, but this cannot happen here because the pyridine nitrogen would have to acquire a permanent positive charge, and

because of the presence of the substituents. So disproportionation occurs instead, and reaction with another BH^+ molecule is proposed by analogy with a similar proposal made for the disproportionation of 4,4'-diiodohydrazobenzene (21, 41). This is likely to be quite a fast reaction, because (a) it is a highly favourable, thermally allowed 14-electron electrocyclic reaction, (b) it is energetically downhill because the aromatic protonated products formed are all much more stable than is **12** in the reaction medium, and (c) formation of three molecules from two counteracts the entropy factor involved in orienting **12** and BH^+ for reaction.

The benzidine rearrangement of hydrazobenzenes is a fast reaction (1). Our reactions are quite fast, but rate comparisons are difficult because most other kinetic studies have been performed in dilute acid media containing a cosolvent, and the acid used is usually HCl or HClO_4 rather than H_2SO_4 (1). The most recent study is that of Bunton and Rubin (48), who studied hydrazobenzene (i.e., 1,2-diphenylhydrazine) and two substituted hydrazobenzenes in pure aqueous HCl and HClO_4 to concentrations of about 1 M; their substrates were diprotonated (on both hydrazo nitrogens), and their reaction rates were much faster than ours, in the stopped-flow range.

Depending on the substrate, the hydrazo group may be diprotonated, monoprotated, or even unprotonated during the rearrangement step, but the process is fastest for diprotonated substrates and slowest for unprotonated ones (1, 21, 48). Our substrates are diprotonated but one of the protons is on the pyridine nitrogen; because of this, protonation on the other hydrazo nitrogen (to give a triprotonated species) is expected to be very difficult, only occurring at acidities much higher than those used here. Diprotonation in hydrazobenzenes is assumed to speed reaction by encouraging N—N bond cleavage and the subsequent charge separation (1). Hydrazo group protonation presumably does that here too, but since the two positive charges are further apart in our case the reaction will not be accelerated nearly so much, which probably accounts for our rates being slower than those of Bunton and Rubin.

Mechanisms are sometimes suggested for the benzidine rearrangement in which the second proton transfer is part of the rate-determining step ($\text{A-S}_{\text{E}2}$ mechanism). For instance, rate-limiting ring carbon protonation followed by fast N—N bond cleavage (47) was a popular mechanism at one time (1), as was rate-determining formation of the $-\overset{+}{\text{N}}\text{H}_2 - \overset{+}{\text{N}}\text{H}_2-$ species with its subsequent rearrangement being a fast process (48). More recent heavy-atom isotope effect results (49) have rendered these mechanisms unlikely, however (21). For the disproportionations in this paper we have good evidence that the second protonation is a pre-equilibrium process (A1 mechanism) and not part of the rate-determining step: the excellent linearity of the Fig. 3 plots, and the fact that the m^\ddagger values (Table 5) are all much greater than one (25).

The $\log k_0$ values in Table 5 fall in the expected order, electron-donor OH fastest, then H, with the electron-withdrawing Cl slowest. The observed $pK_{\text{BH}_2^+}$ values (Table 5) are indicative of only inductive interaction with the positive charge on the hydrazo group; both OH and Cl are inductively electron withdrawing, and both **1** and **10** are more basic than **9**. Any attempted mesomeric interaction of the lone pairs on oxygen with the positive charge on the hydrazo nitrogen leads

to cleavage of the N—N bond as shown at the top of Scheme 13, and this was not observed.

The m^\ddagger values in Table 5 are all quite large, 1.5–1.9, values that are only compatible with an A1 reaction mechanism (25), as discussed. However, they are not all the same; the value for **1**, with a *p*-Cl substituent, is smaller than the others. Variation of m^\ddagger with substituent is not unusual; for instance, a gradual increase with σ^* was observed in *N*-nitro amine decompositions in aqueous H_2SO_4 (27), a slow decrease with σ^+ was seen in some phenylpropionic acid hydrations in these media (50), and slow increases or decreases with σ or σ^+ were found for some acylal and thioacylal hydrolyses (51), and some thiol- and thion-benzoate ester hydrolyses, in aqueous H_2SO_4 (52). What, if anything, these trends mean is not clear at present, although as data accumulate it may become possible to use them for mechanistic diagnosis. It is interesting that Marziano, Tomasin, and Tortato have commented upon similar trends in m^* value in a variety of aqueous acid systems (53), although it is not certain with the data available at present that the aduced variations are real.

Hydroxylation of the (aryloxy)pyridines is an unusual reaction. Normal azobenzenes are stable in strong acid solution, indeed, acidity functions based on their protonation behaviour have been defined (54). Presumably the strongly electron-withdrawing pyridinium substituent in these molecules strongly activates the other ring to nucleophilic attack. The benzidine rearrangement and related processes have always fascinated chemists, and interest in them continues to be high (1, 21–24). For instance, an 18-electron thermally allowed electrocyclic reaction in a benzidine rearrangement has been described very recently (55), which complements the 10- and 14-electron processes discussed in this work. To our knowledge, the work in this paper is the first definitive delineation of the mechanism of the acid-catalyzed benzidine disproportionation reaction as an A1 process.

Acknowledgments

Financial support of this research through a grant by the Natural Sciences and Engineering Research Council of Canada (to E.B.) is gratefully acknowledged. We would also like to thank a referee for helpful comments.

References

1. R.A. Cox and E. Buncl. *In* The chemistry of the hydrazo, azo and azoxy groups. Vol. 1. Edited by S. Patai. Wiley, London, 1975. p. 775.
2. E. Buncl and B.T. Lawton. *Can. J. Chem.* **43**, 862 (1965).
3. E. Buncl and W.M.J. Strachan. *Can. J. Chem.* **48**, 377 (1970).
4. R.A. Cox. *J. Am. Chem. Soc.* **96**, 1059 (1974).
5. R.A. Cox and E. Buncl. *J. Am. Chem. Soc.* **97**, 1871 (1975); E. Buncl, R.A. Cox, and A.J. Dolenko. *Tetrahedron Lett.* 215 (1973); R.A. Cox, A.J. Dolenko, and E. Buncl. *J. Chem. Soc. Perkin Trans. 2*, 471 (1975).
6. E. Buncl. *Acc. Chem. Res.* **8**, 132 (1975).
7. E. Buncl and S.-R. Keum. *J. Chem. Soc. Chem. Commun.* 578 (1983).
8. E. Buncl and S.-R. Keum. *Tetrahedron*, **39**, 1091 (1983).
9. S. Rajagopal and E. Buncl. *Dyes Pigm.* **17**, 303 (1991).
10. E. Buncl and S. Rajagopal. *J. Org. Chem.* **54**, 798 (1989); *Acc. Chem. Res.* **23**, 226 (1990).

11. S.-R. Keum, S.-S. Hur, P.M. Kazmaier, and E. Bunzel. *Can. J. Chem.* **69**, 1940 (1991).
12. S.-R. Keum, K.-B. Lee, P.M. Kazmaier, R.A. Manderville, and E. Bunzel. *Magn. Reson. Chem.* **30**, 1128 (1992).
13. S.-R. Keum, K.-B. Lee, P.M. Kazmaier, and E. Bunzel. *Tetrahedron Lett.* **35**, 1015 (1994).
14. S.-R. Keum, S.-S. Lim, B.-H. Min, P.M. Kazmaier, and E. Bunzel. *Dyes Pigm.* **30**, 225 (1996).
15. S.-R. Keum, P.M. Kazmaier, K.-S. Cheon, R.A. Manderville, and E. Bunzel. *Bull. Korean Chem. Soc.* **17**, 391 (1996).
16. S. Swansburg, Y.-K. Choi, S.-R. Keum, E. Bunzel, and R.P. Lemieux. *Liq. Cryst. In press* (1998).
17. S.-R. Keum, M.-J. Lee, S. Swansburg, E. Bunzel, and R.P. Lemieux. *Dyes Pigm. In press* (1998).
18. E. Bunzel and I. Onyido. *Can. J. Chem.* **64**, 2115 (1986).
19. R. A. Cox, I. Onyido, and E. Bunzel. *J. Am. Chem. Soc.* **114**, 1358 (1992).
20. K.-S. Cheon, R.A. Cox, S.-R. Keum, and E. Bunzel. *J. Chem. Soc. Perkin Trans. 2*, 1231 (1998).
21. R.A. Cox and E. Bunzel. *In The chemistry of the hydrazo, azo and azoxy groups. Vol. 2. Edited by S. Patai. Wiley, London. 1997. p. 569.*
22. D.V. Banthorpe, E.D. Hughes, and C.K. Ingold. *J. Chem. Soc.* 2864 (1964); D. V. Banthorpe. *Top. Carbocycl. Chem.* **1**, 1 (1969); H.J. Shine. *Aromatic rearrangements. Elsevier, Amsterdam. 1967. p. 126; In Mechanisms of molecular migrations. Vol. 2. Edited by B.S. Thyagarajan. Wiley, New York. 1969. p. 191.*
23. H.J. Shine. *J. Phys. Org. Chem.* **2**, 491 (1989); *In Isotopes in organic chemistry. Vol. 8. Edited by E. Bunzel and W.H. Saunders. Elsevier, Amsterdam. 1992. p. 1.*
24. E. Bunzel and K.-S. Cheon. *J. Chem. Soc. Perkin Trans. 2*, 1241 (1998).
25. R.A. Cox. *Acc. Chem. Res.* **20**, 27 (1987); R.A. Cox and K. Yates. *Can. J. Chem.* **57**, 2944 (1979).
26. R.A. Cox. *Can. J. Chem.* **76**, 649 (1998).
27. R.A. Cox. *Can. J. Chem.* **74**, 1774 (1996).
28. R.A. Cox. *J. Chem. Soc. Perkin Trans. 2*, 1743 (1997).
29. R.A. Cox. *Can. J. Chem.* **75**, 1093 (1997).
30. R.A. Cox, D.B. Moore, and R.S. McDonald. *Can. J. Chem.* **72**, 1910 (1994).
31. J.-P. Bégué, F. Benayoud, D. Bonnet-Delpon, A.D. Allen, R.A. Cox, and T.T. Tidwell. *Gazz. Chim. Ital.* **125**, 399 (1995); Y. Chiang, A.J. Kresge, P.A. Obraztsov, and J.B. Tobin. *Croat. Chem. Acta*, **65**, 615 (1992), and earlier papers; M. Lajunen, M. Virta, and O. Kylläinen. *Acta Chem. Scand.* **48**, 122 (1994), and earlier papers.
32. R.A. Cox. *J. Phys. Org. Chem.* **4**, 233 (1991).
33. M. Lajunen, R. Laine, and M. Aaltonen. *Acta Chem. Scand.* **51**, 1155 (1997), and earlier papers.
34. M. Ali and D.P.N. Satchell. *J. Chem. Soc. Perkin Trans. 2*, 167 (1995); *J. Chem. Soc. Perkin Trans. 2*, 1825 (1993).
35. E. Koenigs, W. Freigang, G. Lobmayer, and A. Zscharn. *Ber. Dtsch. Chem. Ges.* **59B**, 321 (1926).
36. C.T. Davis and T.A. Geissman. *J. Am. Chem. Soc.* **76**, 3507 (1954).
37. R.A. Cox and K. Yates. *J. Am. Chem. Soc.* **100**, 3861 (1978).
38. R.A. Cox and K. Yates. *Can. J. Chem.* **59**, 1560 (1981).
39. R.A. Cox, L.M. Druet, A.E. Klausner, T.A. Modro, P. Wan, and K. Yates. *Can. J. Chem.* **59**, 1568 (1981); R.A. Cox and K. Yates. *Can. J. Chem.* **59**, 2116 (1981); *Can. J. Chem.* **62**, 2155 (1984).
40. P.R. Bevington. *Data reduction and error analysis for the physical sciences. McGraw-Hill, New York. 1969. p. 237.*
41. H.J. Shine, J. Habdas, H. Kwart, M. Brechbiel, A.G. Horgan, and J. San Filippo. *J. Am. Chem. Soc.* **105**, 2823 (1983).
42. E. Bunzel and W.M.J. Strachan. *Can. J. Chem.* **47**, 911 (1969).
43. E.-S. Rhee and H.J. Shine. *J. Am. Chem. Soc.* **108**, 1000 (1986).
44. R.A. Cox and K. Yates. *Can. J. Chem.* **59**, 2853 (1981).
45. R.A. McClelland. *Tetrahedron*, **52**, 6823 (1996); J.C. Fishbein and R.A. McClelland. *Can. J. Chem.* **74**, 1321 (1996).
46. M. Novak, M.J. Kahley, J. Lin, S.A. Kennedy, and L.A. Swanegan. *J. Am. Chem. Soc.* **116**, 11626 (1994).
47. G.A. Olah, K. Dunne, D.P. Kelly, and Y.K. Mo. *J. Am. Chem. Soc.* **94**, 7438 (1972).
48. C.A. Bunton and R.J. Rubin. *J. Am. Chem. Soc.* **98**, 4236 (1976).
49. H.J. Shine, G.N. Henderson, A. Cu, and P. Schmid. *J. Am. Chem. Soc.* **99**, 3719 (1977).
50. R.A. Cox, E. Grant, T. Whitaker, and T.T. Tidwell. *Can. J. Chem.* **68**, 1876 (1990).
51. R.A. Cox and K. Yates. *J. Org. Chem.* **51**, 3619 (1986).
52. R.A. Cox and K. Yates. *Can. J. Chem.* **60**, 3061 (1982).
53. N.C. Marziano, A. Tomasini, and C. Tortato. *Org. React. (Tartu)*, **30**, 39 (1996).
54. H.H. Jaffé and R.W. Gardner. *J. Am. Chem. Soc.* **80**, 319 (1958); S.-J. Yeh and H.H. Jaffé. *J. Am. Chem. Soc.* **81**, 3274 (1959); A.J. Kresge and H.-J. Chen. *J. Am. Chem. Soc.* **94**, 8192 (1972).
55. K.H. Park and J.S. Kang. *J. Org. Chem.* **62**, 3794 (1997).